Development 139, 4191-4201 (2012) doi:10.1242/dev.083428

Intercellular calcium signaling in a gap junction-coupled cell network establishes asymmetric neuronal fates in *C. elegans*

Jennifer A. Schumacher[1], Yi-Wen Hsieh[1], Shiuhwei Chen[2], Jennifer K. Pirri[3], Mark J. Alkema[3], Wen-Hong Li[2], Chieh Chang[1,*,‡] and Chiou-Fen Chuang[1,*,‡]

SUMMARY

The *C. elegans* left and right AWC olfactory neurons specify asymmetric subtypes, one default AWC^{OFF} and one induced AWC^{ON}, through a stochastic, coordinated cell signaling event. Intercellular communication between AWCs and non-AWC neurons via a NSY-5 gap junction network coordinates AWC asymmetry. However, the nature of intercellular signaling across the network and how individual non-AWC cells in the network influence AWC asymmetry is not known. Here, we demonstrate that intercellular calcium signaling through the NSY-5 gap junction neural network coordinates a precise 1AWC^{ON}/1AWC^{OFF} decision. We show that NSY-5 gap junctions in *C. elegans* cells mediate small molecule passage. We expressed vertebrate calcium-buffer proteins in groups of cells in the network to reduce intracellular calcium levels, thereby disrupting intercellular communication. We find that calcium in non-AWC cells of the network promotes the AWC^{ON} fate, in contrast to the autonomous role of calcium in AWCs to promote the AWC^{OFF} fate. In addition, calcium in specific non-AWCs promotes AWC^{ON} side biases through NSY-5 gap junctions. Our results suggest a novel model in which calcium has dual roles within the NSY-5 network: autonomously promoting AWC^{OFF} and non-autonomously promoting AWC^{ON}.

KEY WORDS: Gap junctions, Calcium signaling, Stochastic left-right neuronal asymmetry, *C. elegans*

INTRODUCTION

Many cell types communicate through gap junctions during embryonic development to regulate cell-fate determination, proliferation and morphogenesis (Levin, 2007). Gap junctions form intercellular channels that assemble from head-to-head docking of hemichannels, one provided by each of two contacting cells (Bennett and Zukin, 2004). Each hemichannel consists of subunits called connexins and pannexins in vertebrates, and innexins in invertebrates. Gap junction-mediated intercellular communication allows rapid and direct transfer of small molecules and ions across a field of cells without the need for specialized ligands and receptors. Gap junction-mediated calcium waves divide the mammalian neocortex into distinct neuronal domains (Yuste et al., 1995; Bennett and Zukin, 2004). Spontaneous gap junction-dependent calcium waves are also observed in the developing retina (Kandler and Katz, 1998). In addition, gap junction communication through movement of serotonin contributes to orienting the left-right body axis in both frog and avian models (Fukumoto et al., 2005a; Fukumoto et al., 2005b; Levin et al., 2006). Importantly, most studies that defined roles for gap junctions in development relied on broad loss-of-function or inhibition of individual subunits, or global inhibition of molecules that are predicted to pass through gap junctions. Therefore, the roles that individual cells within gap junction networks may play in vivo to drive cell-fate determination or other patterning events are almost completely unknown.

We showed previously that the innexin *nsy-5* (*inx-19* – WormBase) is required for asymmetric differentiation of the *C. elegans* AWC olfactory neuron pair (Chuang et al., 2007). The left and right AWC neurons are morphologically symmetric (White et al., 1986), but express different genes to convey the ability to sense different chemicals (Pierce-Shimomura et al., 2001; Wes and Bargmann, 2001). The two AWC neurons communicate through Notch-independent signaling during late embryogenesis to generate asymmetric cell fates: induced AWC^{ON}, which expresses the reporter gene *str-2p::GFP*, and default AWC^{OFF}, which does not (Troemel et al., 1999; Chuang and Bargmann, 2005). Each wild-type animal generates one AWC^{ON} and one AWC^{OFF}; 50% of the animals induce AWC^{ON} on the left whereas the other 50% induce AWC^{ON} on the right (Troemel et al., 1999). The default AWC^{OFF} fate is executed by the cell-autonomous activity of a calcium/calmodulin-dependent protein kinase II (CaMKII) and mitogen-activated protein kinase (MAPK) cascade (Sagasti et al., 2001; Chuang and Bargmann, 2005). NSY-5 gap junctions and NSY-4 claudins function in parallel to induce AWC^{ON} by inhibiting the CaMKII cascade (VanHoven et al., 2006; Chuang et al., 2007).

nsy-5 is expressed during embryogenesis in both AWC neurons and in at least 17 pairs of other neurons (Chuang et al., 2007) (supplementary material Fig. S1). *nsy-5*-dependent gap junctions transiently connect AWCs and adjacent neurons in embryos. *nsy-5* functions primarily autonomously in AWCs to promote AWC^{ON} fate. However, *nsy-5* activity in ASH, AWB and AFD neurons promotes or inhibits AWC^{ON} (Chuang et al., 2007). These results suggest that individual neighboring neurons in the NSY-5 network, which is defined by the 18 pairs of *nsy-5*-expressing neurons that are likely to be linked by gap junctions (Taylor et al., 2010), communicate with each other and with AWCs to fine-tune the signaling that establishes precise AWC asymmetry. However, the nature of intercellular signaling across the NSY-5 network and how

[1]Division of Developmental Biology, Children's Hospital Medical Center Research Foundation, 240 Albert Sabin Way, Cincinnati, OH 45229, USA. [2]Department of Cell Biology and Biochemistry, University of Texas Southwestern Medical Center at Dallas, 5323 Harry Hines Blvd., Dallas, TX 75390, USA. [3]Department of Neurobiology, LRB 717, University of Massachusetts Medical School, 364 Plantation Street, Worcester, MA 01605, USA.

*These authors contributed equally to this work
‡Authors for correspondence (chiou-fen.chuang@cchmc.org; chieh.chang@cchmc.org)

Accepted 17 August 2012

individual non-AWCs in the network influence AWC asymmetry is not known.

Components of the voltage-gated calcium channel (the pore-forming α1 subunit UNC-2 and the regulatory α2δ subunit UNC-36) are also required upstream of CaMKII for communication between AWCs to ensure a precise $1AWC^{ON}/1AWC^{OFF}$ decision (Bauer Huang et al., 2007). This leads to the hypothesis that intercellular calcium signaling, through NSY-5, mediates communication between AWCs and non-AWCs, and that changes in calcium levels in neurons that are coupled with AWCs through NSY-5 influence AWC fate choice. Here, we develop a unique system to address the roles of specific cells within the NSY-5 network in AWC asymmetry by using cell type-specific expression of calcium-buffering proteins. We show that calcium in non-AWCs of the NSY-5 network is required for the induction of $1AWC^{ON}/1AWC^{OFF}$ asymmetry. In addition, calcium in AWB and ASH neurons confers different side biases of AWC^{ON} induction. Our results support a model in which calcium within the NSY-5 network has dual roles in establishing AWC asymmetry: autonomous promotion of AWC^{OFF} and non-autonomous promotion of AWC^{ON}.

MATERIALS AND METHODS

C. elegans strains

Wild-type strains were *C. elegans* variety Bristol, strain N2. Strains were generated and maintained using standard methods (Brenner, 1974). Integrated transgenic lines and mutations used in these experiments included: *kyIs140 [str-2p::GFP; lin-15(+)] I* (Troemel et al., 1999), *nsy-5(ky634) I* (Chuang et al., 2007), *lfe-2(sy326) I*, *kyIs323 [str-2p::GFP; ofm-1p::GFP] II*, *plc-3(tm1340) II*, *tph-1(mg280) II*, *unc-36(e251) III*, *itr-1(sy331) IV*, *itr-1(sy290) IV*, *itr-1(sy291) IV*, *itr-1(sy327) IV*, *itr-1(sy328) IV*, *nsy-4(ky627) IV* (VanHoven et al., 2006), *unc-43(n498gf) IV*, *eri-1(mg366) IV*, *unc-76(e911) V*, *unc-2(e55) X*, *unc-2(zf35gf) X*, *lin-15b(n744) X*, *ipp-5(sy605) X*, *kyIs136 [str-2p::GFP; lin-15(+)] X*, *vyIs18 [nsy-5p::mCherry-nsy-5 3′]*.

Transgenes maintained as extrachromosomal arrays included: *vyEx498, 499 [odr-3p::calbindin D28K; odr-1p::DsRed; ofm-1p::DsRed]*, *vyEx699, 700 [odr-3p::parvalbumin; odr-1p::DsRed; ofm-1p::DsRed]*, *vyEx1066, 1068, 1069 [odr-3p::calbindin D9K; odr-1p::DsRed; ofm-1p::DsRed]*, *vyEx567, 571 [nsy-5p::calbindin D28K; odr-1p::DsRed; ofm-1p::DsRed]*, *vyEx724, 725, 726 [nsy-5p::parvalbumin; odr-1p::DsRed; ofm-1p::DsRed]*, *vyEx1063 [odr-3p::cmd-1; odr-1p::DsRed; ofm-1p::DsRed]*, *vyEx484 [nsy-5p::calbindin D28K::mCherry; ofm-1p::DsRed]*, *vyEx992, 993, 994, 997 [odr-3p::rParv; odr-1p::DsRed; ofm-1p::DsRed]*, *vyEx990, 991, 996 [odr-3p::rParvCDEF/AV; odr-1p::DsRed; ofm-1p::DsRed]*, *vyEx521, 522 [str-1p::calbindin D28K; odr-1p::DsRed; ofm-1p::DsRed]*, *vyEx562, 564 [sra-6p::calbindin D28K::SL2::mCherry; ofm-1p::DsRed]*, *vyEx568, 569, 570 [str-1p::nsy-5IR::SL2::mCherry; ofm-1p::DsRed]*, *vyEx1320, 1321 [str-1p::mCherry; ofm-1p::DsRed]*, *vyEx1322, 1323 [sra-6p::SL2::mCherry; ofm-1p::DsRed]*.

Plasmid construction and germline transformation

M. musculus calbindin D28K cDNA from pCMV6-calbindin-28K (Origene) was subcloned to make *nsy-5p::calbindin D28K*, *odr-3p::calbindin D28K*, *nsy-5p:calbindin D28K::mCherry*, *str-1p::calbindin D28K* and *sra-6p::calbindin D28K::SL2::mCherry*. *M. musculus* parvalbumin cDNA from pCMV6-parvalbumin (Origene) was subcloned to make *odr-3p::parvalbumin* and *nsy-5p::parvalbumin*. Calbindin D9K cDNA was synthesized from mixed embryonic day (E) 14.5 and postnatal day (P) 0 mouse brain total RNA and subcloned to make *odr-3p::calbindin D9K*. *cmd-1* cDNA was obtained by RT-PCR from L1 stage worms and subcloned to make *odr-3p::cmd-1*. *odr-3p::rParvCDEF/AV* was constructed using the Quikchange II XL Kit (Stratagene). The original construct, rat ParvCDEF, contains four substitutions that replace the first (D51A, D90A) and last (E62V, E101V) charged amino acids of the two EF-hand domains responsible for calcium binding (Pauls et al., 1994; John et al., 2001). We mutated the remaining charged amino acids in the second EF hand domain (K92V, D93A, D95A, K97V and E100V). To make *nsy-5IR*, antisense and sense transcripts of *nsy-5* were inserted upstream and downstream, respectively, of an 888-bp linker sequence as previously described (Chuang and Meyerowitz, 2000). This construct was subcloned to make *str-1p::nsy-5IR::SL2::mCherry*.

odr-3p::calbindin D28K (100 ng/μl), *odr-3p::parvalbumin* (100 ng/μl), *odr-3p::calbindin D9K* (100 ng/μl), *nsy-5p::calbindin D28K* (100 ng/μl), *nsy-5p::parvalbumin* (50 ng/μl), *odr-3p::cmd-1* (50 ng/μl), *nsy-5p::calbindin D28K::mCherry* (100 ng/μl), *odr-3p::rParv* (40 ng/μl), *odr-3p::rParvCDEF/AV* (40 ng/μl), *str-1p::calbindin D28K* (100 ng/μl), *sra-6p::calbindin D28K::SL2::mCherry* (100 ng/μl), *str-1p::nsy-5IR::SL2::mCherry* (100 ng/μl), *str-1p::mCherry* (100 ng/μl), *sra-6p::SL2::mCherry* (100 ng/μl), *odr-1p::DsRed* (15 ng/μl) and *ofm-1p::DsRed* (30 ng/μl) were injected into animals as previously described (Mello and Fire, 1995).

Chemotaxis assays

Chemotaxis assays were performed as previously described (Bargmann et al., 1993). Odors were diluted in ethanol and tested at standard concentrations (1:1000 for butanone and 1:10,000 for 2,3-pentanedione). About 50-200 animals were assayed for each strain and each odor in each individual assay. All assays were performed four independent times. Relative chemotaxis index was calculated by dividing each absolute chemotaxis index by the highest wild-type chemotaxis index observed for each odor for each independent trial.

C. elegans primary cell culture

Cells were isolated from *C. elegans* embryos as previously described (Christensen et al., 2002) and resuspended to a final concentration of 3-7 $\times 10^6$ cells/ml. For dye transfer assays, cells were cultured in rotating eppendorf tubes for 24-48 hours at 22°C prior to assays. For calcium imaging, cells were seeded on 25-mm round cover glasses coated with 0.5 mg/ml peanut lectin (Sigma) and cultures were maintained for 21-72 hours at 22°C in a humidified chamber prior to imaging.

Dye transfer assays

C. elegans embryonic cells were washed twice with HBS (Gibco) containing 10 mM HEPES (pH 7.35) and 5.5 mM glucose, then loaded with 3 μM NPE-HCCC2/AM (plus 0.015% puronic acid in 0.015% DMSO) for 45 minutes in the dark at 22°C. Loaded cells were washed with HBS and seeded on 15-mm slides that had been precoated with peanut lectin (Sigma), in 35-mm dishes (MatTek). Seeded cells were incubated in HBS for 15 minutes to allow complete hydrolysis of acetoxymethyl (AM) esters. Localized ultraviolet (UV) uncaging of NPE-HCCC2 and fluorescence imaging were performed on an inverted Zeiss Axiovert 200 with a Hamamatsu ORCA-ER cooled CCD camera and 100× oil immersion objective (NA 1.4) as previously described (Dakin et al., 2005). Images were acquired and analyzed with the Openlab integrated imaging software (Improvision). All of the five wild-type cell pairs that were analyzed showed dye transfer, whereas none of the five *nsy-5(lf)* cell pairs assayed had dye transfer.

Calcium imaging

C. elegans embryonic cells were loaded with Fluo-4 calcium-indicator dye as previously described (Marsh, 1995). Briefly, cells were washed three times with physiological saline solution (PSS; 145 mM NaCl, 5 mM KCl, 1 mM $MgSO_4$, 10 mM HEPES, pH 7.4, 10 mM glucose, plus 2 mM $CaCl_2$), then loaded with 1.5 μM Fluo-4, AM (plus 0.015% puronic acid in 0.015% DMSO) for 45 minutes in the dark at 22°C. Cells were washed three times with PSS (2 mM $CaCl_2$), then recovered in the final wash for 30-60 minutes in the dark. Ionomycin (in PSS plus 10 mM $CaCl_2$) was added on top of cells to a final concentration of 10 μM. EGTA in PSS was added on top of cells to a final concentration of 6 mM. Optical recording was performed using an Olympus IXS1 inverted microscope equipped with a Hamamatsu ORCA-AG camera. Frames were acquired at 2-second intervals for a total of 4 minutes. Images were processed using ImageJ software. At each time point, Fluo-4 fluorescence was normalized to mCherry fluorescence.

Genetic mosaic analysis

Mosaic analysis and statistical analysis were performed as previously described (Sagasti et al., 2001; VanHoven et al., 2006; Chuang et al., 2007). For experiments using the *str-1* and *sra-6* promoters, bicistronic constructs were generated using the SL2 trans-splicing signal to drive both the gene of interest and mCherry, and mCherry expression determined retention of the transgenes. Previous studies showed that the *nsy-5* promoter, *odr*-3 promoter, *str-1* promoter, *sra-6* promoter, *odr-1p::DsRed* and various co-injection markers had no effect on *str-2::GFP* expression (Sagasti et al., 2001; Chuang and Bargmann, 2005; VanHoven et al., 2006; Bauer Huang et al., 2007; Chuang et al., 2007). At least two independent lines of the same transgene were analyzed. Expected numbers of mosaic animals were predicted from non-mosaic animals of the same transgenic line.

RESULTS

NSY-5 gap junctions mediate small molecule transfer between *C. elegans* embryonic neurons

Consistent with its cell-intrinsic and network functions in AWC asymmetry, NSY-5 can form both functional hemichannels and intercellular gap junction channels in *Xenopus* oocytes (Chuang et al., 2007). However, the permeability properties of NSY-5 gap junctions in *C. elegans* have not been examined. To determine the permeability of NSY-5 gap junctions to small molecules in *C. elegans* embryonic cells, we used a photoactivatable (caged) fluorescent dye and the uncaging/imaging technique (Dakin et al., 2005; Dakin and Li, 2006). Embryonic neurons were isolated from *nsy-5p::mCherry* transgenic animals, in which neurons of the NSY-5 network were labeled with mCherry (Shaner et al., 2004; Shaner et al., 2005). Cultured neurons were loaded with the cell-permeable caged fluorophore NPE-HCCC2/AM (Zhao et al., 2004; Dakin et al., 2005). After entering the cell, the acetoxymethyl (AM) esters are hydrolyzed and the caged dye (NPE-HCCC2) becomes trapped inside the cell. When uncaged by UV light, the parent fluorophore HCCC2 is released. As the molecular weight of HCCC2 is 450 Da, well below the ~1.2 kDa molecular passage limit of typical gap junction channels (Kumar and Gilula, 1996), HCCC2 diffuses to its neighboring cells through gap junctions (Fig. 1A). We focused on pairs of *nsy-5p::mCherry*-expressing cells that made direct contact (Fig. 1B,C,I,J), and uncaged the fluorophore in one cell. In wild-type cell pairs, HCCC2 transferred rapidly from the uncaged cell (donor) to its neighboring cell (recipient) (Fig. 1E-H). By contrast, in cell pairs isolated from *nsy-5* loss-of-function (lf) embryos, in which *nsy-5*-dependent gap junctions were absent (Chuang et al., 2007), fluorescent HCCC2 was only detected in the uncaged cell (cell 1) and no fluorescence was observed in its

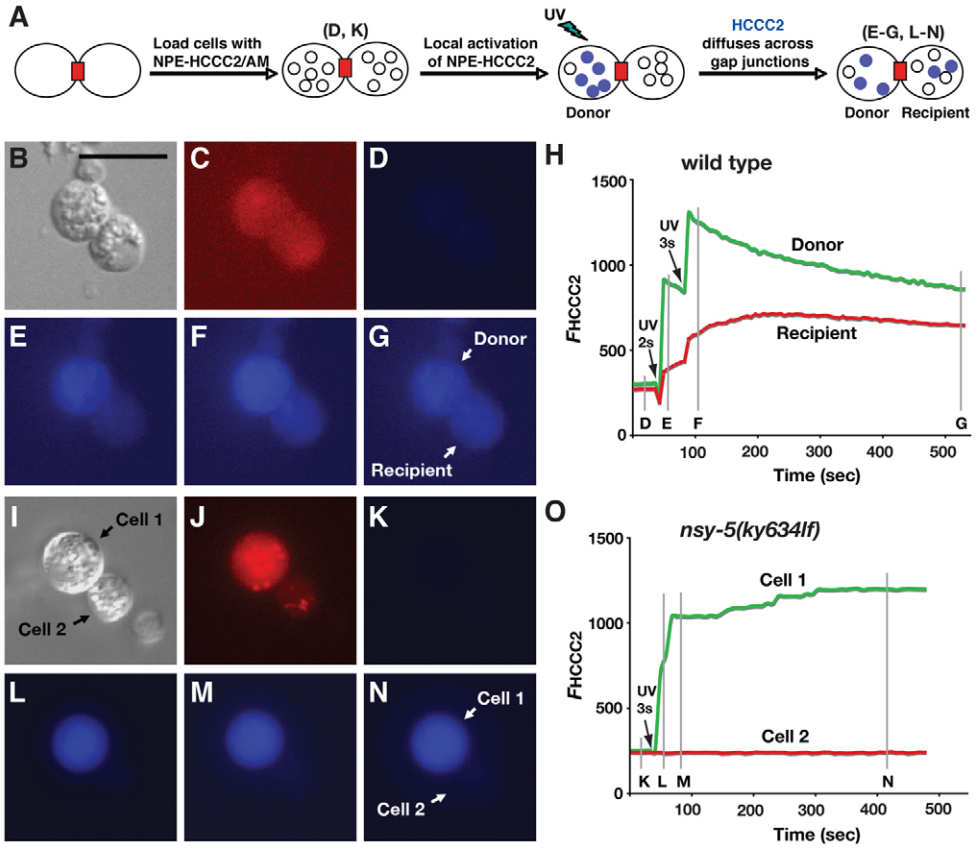

Fig. 1. NSY-5 gap junctions mediate small dye transfer between *C. elegans* embryonic neurons. (**A**) Schematic of the dye transfer technique. Black open circles, NPE-HCCC2; blue dots, HCCC2; red rectangles, gap junctions. (**B-G**) One pair of *nsy-5p::mCherry* cells from wild-type embryos. (B) Differential interference contrast (DIC) and (C) mCherry images. (D-G) Images of fluorescent HCCC2 in the coupled cells prior to UV (360 nm) uncaging (D), immediately after the first (E) and second (F) localized uncaging of one cell (donor), and when the transfer of fluorescent HCCC2 from donor cell to recipient cell reached equilibrium (G). (**H**) Time course of fluorescence intensities of HCCC2 (F_{HCCC2}) in the wild-type coupled cells. D, E, F and G indicate the time points at which the images in D, E, F and G, respectively, were acquired. (**I-N**) One pair of *nsy-5p::mCherry*-expressing cells from *nsy-5(ky634lf)* embryos. (I) DIC and (J) mCherry images. (K-N) Images of fluorescent HCCC2 before localized uncaging of cell 1 (K), immediately after uncaging (L) and 40 seconds (M) and 380 seconds (N) after uncaging. (**O**) Time course of fluorescence intensities of HCCC2 (F_{HCCC2}) in the *nsy-5(lf)* cell pair. K, L, M and N indicate the time points at which the images in K, L, M and N, respectively, were acquired. Scale bar: 10 μm.

neighboring cell (cell 2) (Fig. 1L-O). These results indicate that NSY-5 gap junctions can mediate small molecule transfer between coupled *C. elegans* neurons.

Expression of vertebrate calcium buffers proteins in a subset of NSY-5 network cells disrupts AWC asymmetry

To determine the requirements for intracellular free calcium in specific cells within the NSY-5 network, we established transgenic lines expressing the vertebrate calcium-buffer proteins calbindin D28K, parvalbumin or calbindin D9K in various subsets of neurons. Calcium-buffer proteins contain EF-hand domains (four functional domains in calbindin D28K and two each in parvalbumin and calbindin D9K) responsible for binding to and sequestering intracellular free calcium, preventing calcium from activating downstream targets such as CaMKII (Ikura, 1996). There are no homologs of these calcium buffer genes in the *C. elegans* genome (*C. elegans* Sequencing Consortium, 1998).

Expression of each buffer under the control of the *odr-3* promoter (Roayaie et al., 1998), which is strongly expressed in AWC and weakly in AWB neurons, led to *str-2::GFP* expression in both AWC neurons (2AWC^{ON} phenotype) (Fig. 2D,E; supplementary material Table S1), in contrast to the 1AWC^{OFF}/1AWC^{ON} phenotype observed in the wild-type population (Fig. 2A,E). The 2AWC^{ON} phenotype is identical to the loss-of-function mutant phenotype of the calcium channel α2δ subunit gene *unc-36* (Troemel et al., 1999) (Fig. 2C,E; supplementary material Table S1), consistent with each buffer strongly inhibiting calcium signaling. Mutations of conserved charged residues at the beginning and end of the two EF-hand calcium-binding domains of parvalbumin reduce calcium binding in vitro (Pauls et al., 1994). To determine whether parvalbumin generates a 2AWC^{ON} phenotype owing to its ability to bind calcium, we mutated all charged resides in the second EF-hand domain. This resulted in a significant reduction of 2AWC^{ON} phenotype (P=0.006, n=245), suggesting that the 2AWC^{ON} phenotypes are specifically due to calcium-binding activity.

nsy-5 mutants have two AWC^{OFF} cells (2AWC^{OFF} phenotype) (Chuang et al., 2007) (Fig. 2B,E), consistent with the requirement of gap junction-mediated signaling for AWC^{ON} induction. Calbindin D28K or parvalbumin expression in the entire NSY-5 network resulted in 2AWC^{ON}, but also significantly increased the percentage of 2AWC^{OFF} compared with expression primarily in AWCs (Fig. 2E; supplementary material Table S1), suggesting that intracellular calcium signals in non-AWCs of the NSY-5 network promotes the wild-type 1AWC^{ON}/1AWC^{OFF} phenotype.

odr-3p::calbindin D28K animals chemotaxed normally to butanone, which is sensed by the AWC^{ON} cell, but did not chemotax to 2,3-pentanedione, which is sensed by the AWC^{OFF} cell (Fig. 2F). These results confirm that the AWC^{OFF} cell fate is lost in *odr-3::calbindin D28K* animals, and that the AWC^{ON} cells are capable of performing an appropriate physiological function. Because calbindin D28K has the highest number (four) of potential calcium-binding sites among the calcium-buffer proteins, we focused primarily on developing this buffer as a tool to examine the role of calcium in specific cells in the NSY-5 network.

Calbindin D28K acts as a calcium buffer in NSY-5 network neurons

Calcium-buffer proteins share the EF-hand calcium-binding domain with calcium sensors, which bind to calcium and promote signaling by activating downstream kinase cascades. Although it

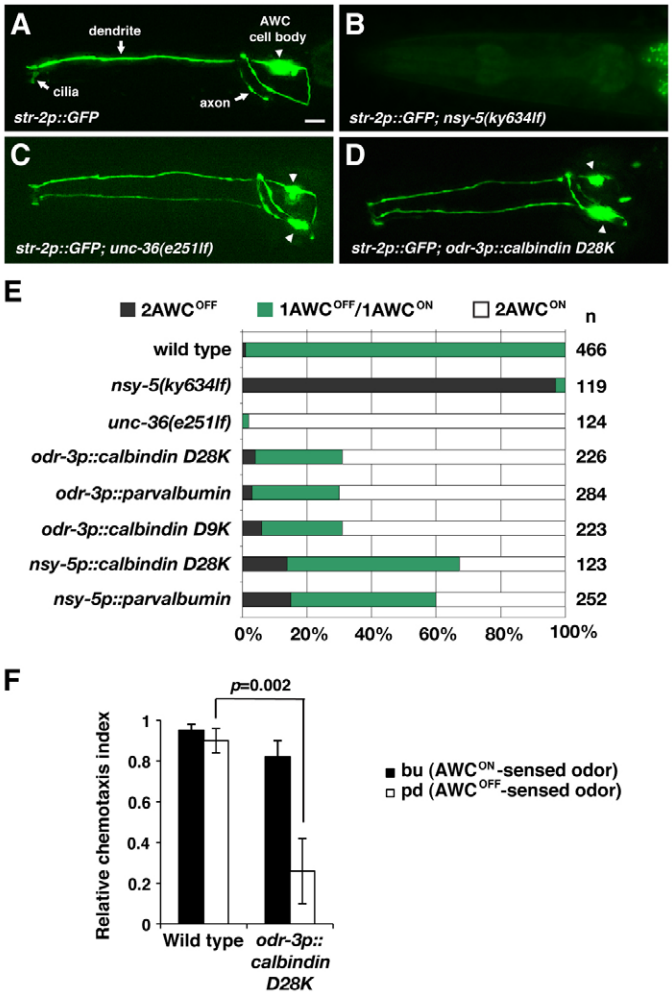

Fig. 2. Calcium buffer expression in the NSY-5 network disrupts AWC asymmetric gene expression and function. (**A-D**) Expression of the reporter gene *str-2p::GFP* in wild type (A), *nsy-5(ky634lf)* (B), *unc-36(e251lf)* (C) and *odr-3p::calbindin D28K* transgenic worms (D). Anterior is left; ventral is down. Arrowheads indicate AWC cell bodies. Scale bar: 10 μm. (**E**) AWC phenotypes of wild type, mutants and calcium buffer-expressing animals. (**F**) Mean relative chemotaxis indices. Wild-type animals are non-transgenic siblings from *odr-3p::calbindin D28K* extrachromosomal arrays. bu, 1:1000 butanone; pd, 1:10,000 2,3-pentanedione. Significance was calculated using *t*-test. Error bars indicate s.e.m.

is well established that calbindin D28K and parvalbumin function as calcium buffers in vertebrate systems and transgenic fly neurons (Chard et al., 1993; Grabarek, 2006; Harrisingh et al., 2007), their calcium-buffering ability has not been tested in any type of *C. elegans* cells. *unc-43*/CaMKII gain-of-function (gf) mutants have a 2AWC^{OFF} phenotype (Troemel et al., 1999) (Fig. 3A; supplementary material Table S1). To confirm that calbindin D28K does not promote calcium signaling, we compared the abilities of calbindin D28K and *C. elegans* CMD-1/calmodulin, a calcium sensor that activates CaMKII, to induce a 2AWC^{OFF} phenotype. Neither protein when expressed alone in AWCs under the *odr-3* promoter strongly induced a 2AWC^{OFF} phenotype (Fig. 3A; supplementary material Table S1). Calcium concentration could be one of the limiting factors in allowing *cmd-1* to activate

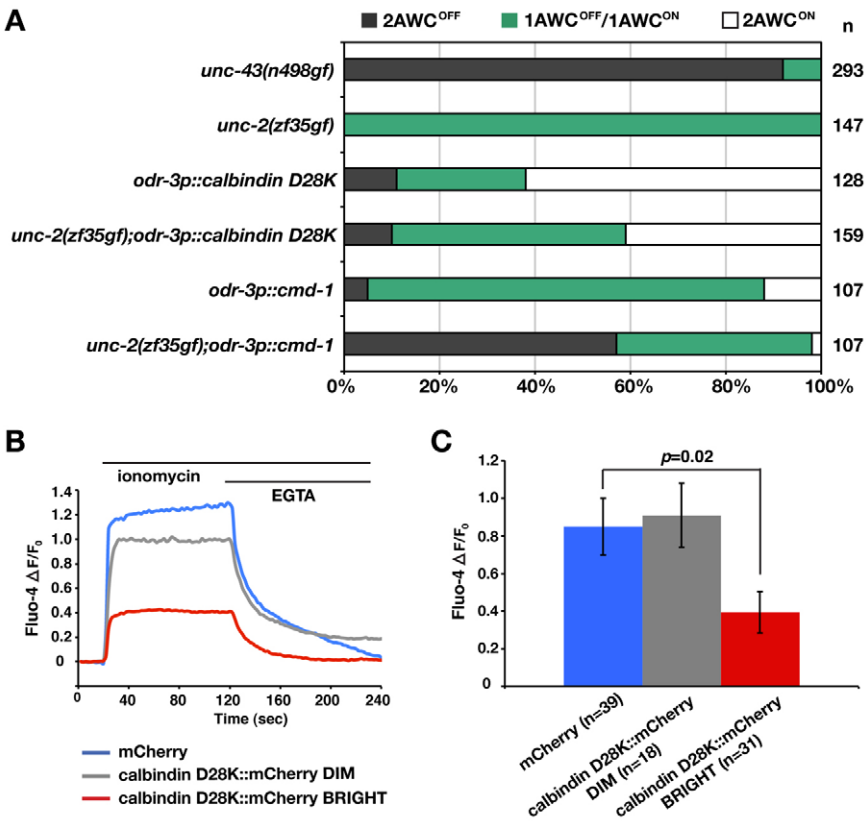

Fig. 3. Calbindin D28K acts as an intracellular calcium buffer in NSY-5 network embryonic neurons. (**A**) AWC phenotypes of calcium buffer (*odr-3p::calbindin D28K*) and calcium sensor (*odr-3p::cmd-1*) expressing animals alone or in the *unc-2(zf35gf)* background. (**B**) Representative traces of calcium dynamics in cultured *C. elegans* embryonic neurons during addition of the stimulus (ionomycin) followed by calcium chelator (EGTA). Horizontal lines indicate the duration of ionomycin and EGTA application. ΔF, the change in Fluo-4 fluorescence; F_0, the resting Fluo-4 fluorescence prior to ionomycin stimulation. (**C**) Average maximum change in Fluo-4 intensity following ionomycin application. Significance was calculated using *t*-test. Error bars indicate s.e.m.

downstream targets. *unc-2(zf35)* is a gain-of-function allele of the neuronal P/Q type calcium channel (J.K.P. and M.J.A., unpublished), which should lead to a rise in intracellular calcium. Although *unc-2(zf35gf)* mutants had wild-type AWC asymmetry (Fig. 3A; supplementary material Table S1), they may provide a sensitized background for a 2AWC^{OFF} phenotype. When the same *odr-3p::calbindin D28K* or *odr-3p::cmd-1* transgenes were expressed in *unc-2(zf35gf)* homozygous mutants, *odr-3p::cmd-1* generated a strong 2AWC^{OFF} phenotype (Fig. 3A; supplementary material Table S1), indicative of promoting calcium signaling. Importantly, *odr-3p::calbindin D28K* did not promote 2AWC^{OFF} in the *unc-2(zf35gf)* background (Fig. 3A), indicating that calbindin D28K does not activate downstream targets and supporting the role of calbindin D28K as a calcium buffer rather than a calcium sensor.

To confirm that calbindin D28K reduces the amount of intracellular free calcium, we performed calcium-imaging experiments in *C. elegans* primary cell culture. We targeted neurons in the NSY-5 network by expressing mCherry or calbindin D28K::mCherry translational fusion protein under the control of the *nsy-5* promoter. The *nsy-5p::calbindin D28K::mCherry* transgene allowed us to determine relative levels of calbindin D28K expression in each cell, which we broadly categorized into 'dim' cells, which had lower levels of calbindin D28K, and 'bright' cells, which had higher levels of calbindin D28K. Wild-type mCherry-expressing neurons displayed a typical increase in intracellular calcium measured by the calcium indicator Fluo-4 following ionomycin (a calcium ionophore) application (Fig. 3B,C). 'Dim' calbindin D28K::mCherry neurons had a similar increase to wild-type neurons (Fig. 3B,C). However, the increase in intracellular calcium was significantly reduced in 'bright' neurons, which expressed high levels of calbindin D28K::mCherry, indicating that calbindin D28K is able to bind and sequester intracellular calcium. Taken together, these results are consistent with calbindin D28K acting as a calcium buffer in the NSY-5 network to disrupt AWC asymmetry.

Calcium buffers antagonize the *unc-2/unc-36* calcium signaling pathway

The 2AWC^{ON} phenotype caused by calcium buffer expression in AWCs resembles that seen in loss-of-function mutations of *unc-2* and *unc-36* calcium channels and of the downstream calcium-activated *unc-43* (CaMKII)/*tir-1* (Sarm1 adaptor)/*nsy-1* (MAPKKK) kinase pathway (Troemel et al., 1999; Sagasti et al., 2001; Chuang and Bargmann, 2005; Chang et al., 2011) (Fig. 4A,B). This similarity suggests that the calcium buffer-induced 2AWC^{ON} phenotype could result from an inhibition of the *unc-2/unc-36* calcium signaling pathway.

To determine the relationship between the calcium-buffer target and other genes affecting AWC asymmetry, we crossed *odr-3p::calbindin D28K* or *odr-3p::parvalbumin* transgenic animals (2AWC^{ON}) with 2AWC^{OFF} mutants. Loss-of-function mutations in the *unc-76* axon outgrowth gene, the *nsy-5* innexin gene and the *nsy-4* claudin-like gene, or gain-of-function mutations in the *unc-43* CaMKII gene cause a 2AWC^{OFF} phenotype (Troemel et al., 1999; VanHoven et al., 2006; Chuang et al., 2007) (Fig. 4A,B). Calbindin D28K or parvalbumin expression strongly suppressed the 2AWC^{OFF} phenotype of *unc-76(lf)*, *nsy-5(lf)* or *nsy-4(lf)* mutants (Fig. 4A), indicating that calcium buffers function downstream of axon outgrowth, *nsy-5* and *nsy-4* (Fig. 4B). By contrast, the 2AWC^{ON} phenotype resulting from calbindin D28K or parvalbumin expression was greatly suppressed by *unc-43* gain-of-function mutants (Fig. 4A), suggesting that calcium buffers act on a target predominantly upstream of *unc-43* (Fig. 4B).

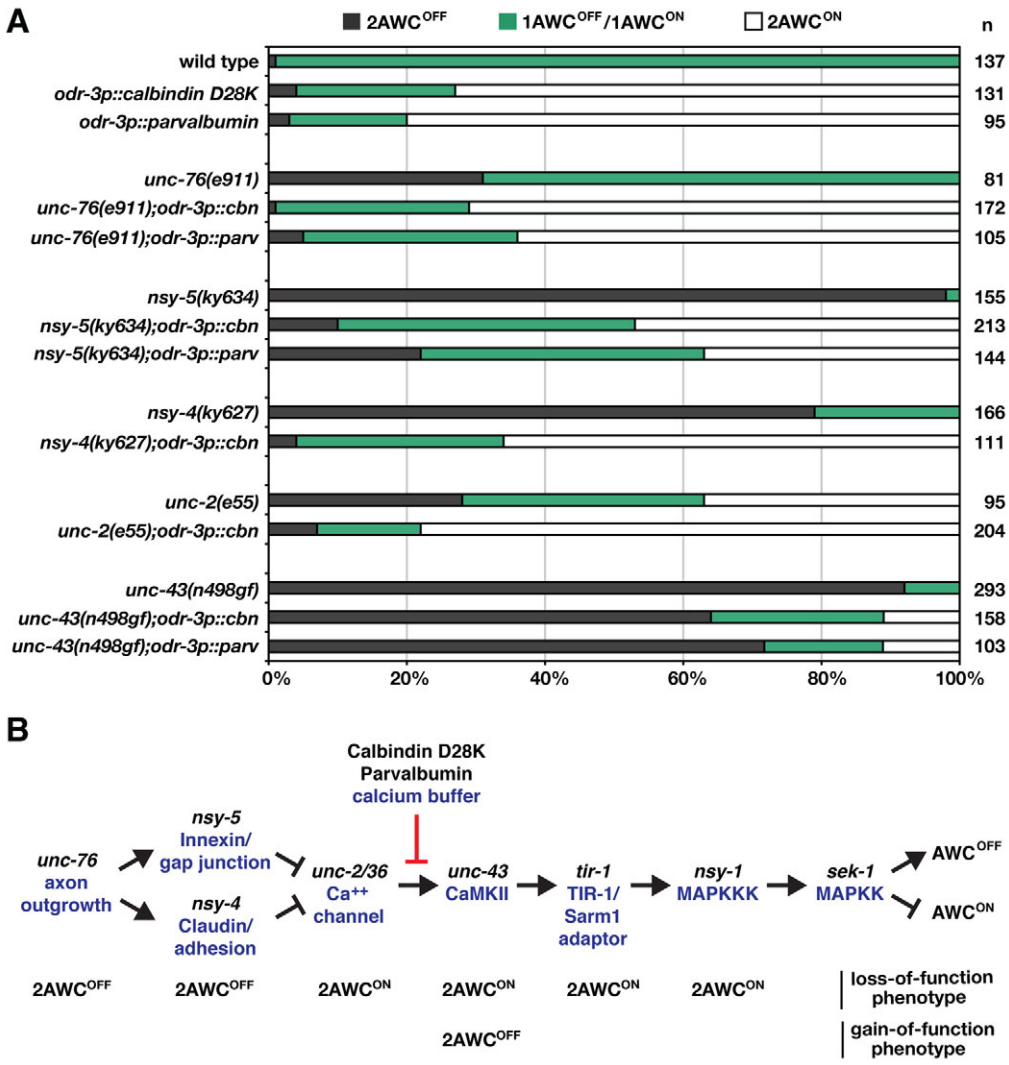

Fig. 4. Calcium buffers antagonize the *unc-2/unc-36* calcium signaling pathway. (**A**) AWC phenotypes of animals expressing calcium buffers alone or in mutants defective in AWC asymmetry. cbn, calbindin D28K; parv, parvalbumin. (**B**) The AWC asymmetry determination pathway.

These results suggest that calcium buffers affect the AWC signaling step downstream of *nsy-5* and *nsy-4*, and upstream of *unc-43*. Previous genetic studies suggest that *unc-2* and *unc-36* calcium channels also act downstream of *nsy-5* and *nsy-4*, and upstream of *unc-43* (Troemel et al., 1999; VanHoven et al., 2006; Chuang et al., 2007). Thus, we examined the genetic interaction between the calcium-buffer target and *unc-2*. The *unc-2(e55)* mutant had a mixed 2AWC^{ON} and 2AWC^{OFF} phenotype due to functional redundancy of *unc-2* with the additional α1 subunit *egl-19* and inhibition of *egl-19* activity by *unc-2*, respectively (Troemel et al., 1999; Bauer Huang et al., 2007) (Fig. 4A). Calbindin D28K expression significantly suppressed the 2AWC^{OFF} phenotype of *unc-2(e55)* mutants (Fig. 4A). Together, these results are consistent with the antagonistic effect of calcium buffers on the *unc-2/unc-36* calcium signaling pathway (Fig. 4B).

Intracellular calcium acts cell-autonomously in AWCs to promote AWC^{OFF}

Based on previous results that calcium-signaling components (*unc-43*, *tir-1*, *nsy-1*) function cell-autonomously to execute the AWC^{OFF} fate (Sagasti et al., 2001; Chuang and Bargmann, 2005), we hypothesized that the calcium buffers would cell-autonomously inhibit the calcium-signaling pathway to promote AWC^{ON}. To test this hypothesis, we performed genetic mosaic analysis using calbindin D28K transgenes expressed primarily in AWCs and AWBs using the *odr-3* promoter. Transgenes are inherited as extrachromosomal arrays that are unstable and subject to spontaneous mitotic loss in random cell lineages. Mosaic animals were identified by loss of the co-injection marker *odr-1p::DsRed*, which is expressed in AWC left (AWCL), AWC right (AWCR), AWB left (AWBL) and AWB right (AWBR). These four cells represent four lineage groups within the NSY-5 network (Chuang et al., 2007) (supplementary material Fig. S1), and thus can serve as indicators of which cells within the network retain or lose calbindin D28K transgenes. Seventy percent of non-mosaic calbindin D28K animals had 2AWC^{ON} (Fig. 5B; Table 1, row d). Non-mosaic 1AWC^{ON} animals showed no side bias of AWC^{ON} induction. In >90% of mosaic animals that retained the calcium buffer only in one AWC, the calcium-buffered AWC became AWC^{ON} and the wild-type AWC became AWC^{OFF}, independent of expression of the buffer in AWB cells (Fig. 5C; Table 1, rows e,f). This suggests that intracellular calcium is required cell-autonomously to execute AWC^{OFF} cell-fate specification (Fig. 6A).

Intracellular calcium signals in non-AWCs promotes 1AWC^{ON}/1AWC^{OFF}

Based on our observation that expressing the buffers in the entire NSY-5 network led to a moderate 2AWC^{OFF} phenotype (Fig. 2E),

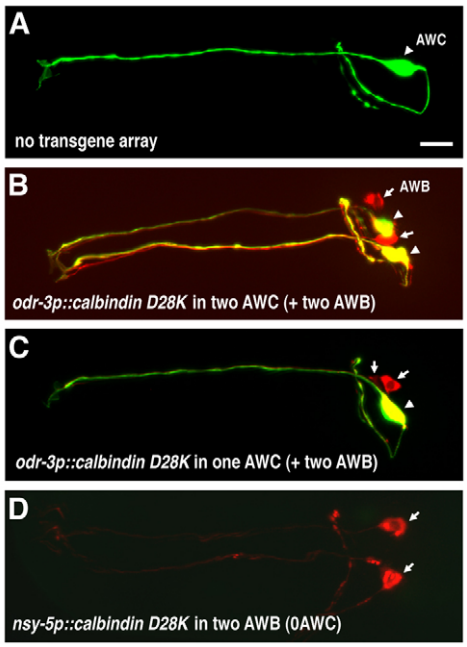

Fig. 5. Calcium acts autonomously in AWCs to promote AWC^{OFF} and non-autonomously in non-AWCs to promote AWC^{ON}. (**A-D**) Expression of an integrated *str-2p::GFP* transgene and an unstable transgenic array bearing *odr-3p::calbindin D28K* or *nsy-5p::calbindin D28K* and the mosaic marker *odr-1p::DsRed* in non-transgenic (A), non-mosaic (B) and representative mosaic (C,D) worms. AWC neurons that express both GFP and DsRed appear yellow. (C) Mosaic animal that retains *odr-3p::calbindin D28K* in AWCL. (D) Mosaic animal that lost *nsy-5p::calbindin D28K* in both AWCs but retained the transgene in both AWBs. Arrowheads indicate AWC cell bodies; arrows indicate AWB cell bodies. Anterior is left; ventral is down. Scale bar: 10 μm.

we hypothesized that calcium within non-AWC cells is required to promote 1AWC^{ON}/1AWC^{OFF}. To test this hypothesis, we performed mosaic analysis with the *nsy-5p::calbindin D28K; odr-1p::DsRed* transgenic extrachromosomal arrays to determine whether buffering calcium only in non-AWC neurons within the NSY-5 network was able to disrupt asymmetry. As 15 out of the 34 non-AWC cells expressing *nsy-5* are closely related to either AWB by lineage (Chuang et al., 2007) (supplementary material Fig. S1), their genotypes can be inferred by following the *odr-1p::DsRed* expression in AWB. If calcium signaling in non-AWC cells is required for AWC^{ON} induction, buffering of calcium signals in the AWB lineage would disrupt intercellular calcium signaling within the NSY-5 network and lead to a defect in the induction of AWC^{ON} fate. Thus, we examined mosaic animals that had *odr-1p::DsRed* expression in both AWB cells but not in either AWC, which would have buffered calcium levels in ~50% of non-AWCs in the NSY-5 network. Interestingly, 79% of this type of mosaic animals had 2AWC^{OFF} (Fig. 5D; Table 1, row c). In addition, we examined *odr-3p::calbindin D28K* mosaic animals that retained the array only in both AWC cells, and found that only 38% of animals had 2AWC^{ON} (Table 1, row g), compared with 70% when calcium was buffered in both AWCs and AWBs (Table 1, row d). These results support the hypothesis that intracellular calcium in non-AWC cells of the NSY-5 network is required to promote 1AWC^{ON}/1AWC^{OFF} (Fig. 6B; supplementary material Fig. S2A).

Calcium in AWB and ASH contributes to AWC^{ON} side bias

To refine the requirements of calcium in the AWB lineage further, we examined the role of calcium in AWBs. We examined mosaic animals that lost the *odr-3p::calbindin D28K* array only in AWBL or AWBR, and determined whether AWCL or AWCR becomes AWC^{ON}. Of the 1AWC^{ON} mosaic animals that lost the *odr-3p::calbindin D28K* array in AWBR, 74-77% had a significant bias towards the opposite side AWCL becoming AWC^{ON}, regardless of the presence of the transgene in both AWCs (Table 1, rows h,j). Because AWB inhibits AWC^{ON} fate via NSY-5 (Chuang et al., 2007), these results are consistent with the hypothesis that normal calcium levels in AWBR inhibits AWCR from becoming AWC^{ON}. In the *nsy-5(lf)* mutant, mosaic animals that lost the array in AWBR no longer had a bias towards AWCL^{ON} (Table 1, rows j,m), suggesting that calcium in AWBR requires gap-junction communication within the NSY-5 network to inhibit AWCR^{ON}. In addition, this result supports the notion that calcium travels through NSY-5 gap junctions within the network.

To probe the role for AWB further, we used the *str-1* promoter (Troemel et al., 1997) to drive expression of calbindin D28K only in AWB. Expression of *str-1p::calbindin D28K* in both AWBL and AWBR did not disrupt AWC asymmetry (Table 1, row n; supplementary material Table S1), whereas the similar class of animals containing the *nsy-5p::calbindin D28K* array did disrupt AWC asymmetry (Table 1, row c). These results suggest that other cells in the AWB lineage of the NSY-5 network also contribute to promoting the wild-type 1AWC^{ON}/1AWC^{OFF} fate. Mosaic animals that lost *str-1p::calbindin D28K* in AWBR had a significant bias towards AWCL^{ON} (Table 1, row o), confirming that the negative influence on AWCR^{ON} via calcium is partly, if not completely, derived from AWBR (supplementary material Fig. S2B). Control mosaic experiments showed that *str-1p::mCherry* did not influence AWC^{ON} side bias (supplementary material Table S2). To test whether *nsy-5*, like calcium, in AWBR generates AWCL^{ON} side bias, we made a tissue-specific inverted repeat (IR) RNAi construct, *str-1p::nsy-5IR*. Knocking down NSY-5 in both AWBL and AWBR did not disrupt AWC asymmetry or generate an AWC^{ON} side bias (Table 1, row q). Consistent with our *str-1p::calbindin D28K* results (Table 1, row o), 62% of 1AWC^{ON} animals that lost *str-1p::nsy-5IR* in AWBR had a significant bias towards AWCL^{ON} (Table 1, row r). These results suggest that the negative influence of AWBR on AWCR^{ON} is dependent on both calcium and *nsy-5*. In addition, 70% of 1AWC^{ON} animals that lost *str-1p::nsy-5IR* in AWBL had a significant bias towards AWCR^{ON} (Table 1, row s). As the same class of mosaic animals containing the *str-1p::calbindin D28K* did not show a bias towards AWCR^{ON} (Table 1, row p), these results suggest that other signals from AWBL might go through NSY-5 gap junctions to negatively influence AWCL^{ON}.

ASH neurons are derived from the same lineage as AWCs. To examine whether calcium in ASH generates AWC^{ON} side bias, we used the *sra-6* promoter (Troemel et al., 1995) to drive calbindin D28K expression primarily in ASH, in addition to ASI neurons. Expression of *sra-6p::calbindin* D28K in both ASH and ASI did not disrupt AWC asymmetry nor did it generate AWC^{ON} side bias (Table 1, row t; supplementary material Table S1). Mosaic animals that lost the array in ASHL had a significant bias towards AWCL^{ON} (Table 1, row v). Control mosaic experiments showed that *sra-6p::SL2::mCherry* did not influence AWC^{ON} side bias (supplementary material Table S2). ASH was previously shown to promote AWC^{ON} fate via NSY-5 (Chuang et al., 2007), suggesting

Table 1. Individual neurons in the NSY-5 network play specific roles in influencing AWC^{ON} fate and side bias

Genetic background	Transgene array	Row	Cells with transgene array				*str-2p::GFP* phenotype (%)				
			AWCL	AWCR	AWBL	AWBR	2AWC^{OFF}	AWCL^{ON}	AWCR^{ON}	2AWC^{ON}	*n*
Wild type	*nsy-5p:: calbindin D28K*	a	–	–	–	–	0	46	54	0	254
		b	+	+	+	+	10	20 (49)	21 (51)	49	1266 (519)
		c	–	–	+	+	**79******[b]	4	17	0	29
	odr-3p:: calbindin D28K	d	+	+	+	+	2	13 (46)	15 (54)	70	1492 (418)
		e	–	+	+/–	+/–	7	2	91 (**98**)****[d]	0	109 (101)
		f	+	–	+/–	+/–	6	90 (**96**)****[d]	4	0	99 (93)
		g	+	+	–	–	0	33	29	**38*****[d]	24
		h	–	–	+	–	0	**77****[d]	23	0	22
		i	–	–	–	+	0	80	20	0	5
		j	+	+	+	–	1	28 (**74**)****[d]	10 (26)	61	171 (65)
		k	+	+	–	+	3	14	16	67	154
nsy-5(ky634)	*odr-3p:: calbindin D28K*	l	+	+	+	+	12	18 (47)	20 (53)	50	1224 (465)
		m	+	+	+	–	9	26 (51)[ns l]	25 (49)	39	214 (110)
Wild type	*str-1p:: calbindin D28K*	n			+	+	3	38 (39)	59 (61)	0	1258 (1220)
		o			+	–	0	**58****[n]	42	0	62
		p			–	+	0	35	65[ns n]	0	57
	str-1p:: nsy-5IR	q			+	+	4	44 (46)	52 (54)	0	445 (427)
		r			+	–	4	59 (**62**)**[q]	37 (38)	0	76 (73)
		s			–	+	6	28 (30)	66 (**70**)*[q]	0	61 (57)
			ASHL	ASHR	ASIL	ASIR					
Wild type	*sra-6p:: calbindin D28K*	t	+	+	+	+	1	43	56	0	425
		u	+	–	+/–	+/–	0	53	47	0	45
		v	–	+	+/–	+/–	2	59 (**60**)**[t]	39 (40)	0	69 (68)
		w	+	+	+	–	0	25	**75****[t]	0	55
		x	+	+	–	+	4	49	47	0	51

The *odr-3p::calbindin D28K; odr-1p::DsRed* transgene analyzed in rows d-k was crossed into the *nsy-5(ky634lf)* mutant for the analysis in rows l, m.
The *str-1p::nsy-5IR::SL2::mCherry* transgene was analyzed in the RNAi-sensitive strain *eri-1(mg366); lin-15B(n744)* (Sieburth et al., 2005).
+, cells that retain the array; –, cells that lost the array; *n*, number of animals characterized.
cbn, calbindin D28K.
Data in parentheses are the percentages or numbers of animals with AWCL^{ON} and AWCR^{ON}, calculated when the data of 2AWC^{OFF} and 2AWC^{ON} phenotypes are excluded.
Values in bold are significantly different from the expected values in the same column (row indicated by [b,d,l,n,q,t]). Significance was calculated using *Z*-test for two proportions.
*****P*<0.0001; ****P*=0.001; ***P*<0.01 (rows h, o, v, w) or ***P*=0.01 (row r); **P*=0.02; ns, not significant.

that calcium in ASHL promotes AWCL^{ON} fate (supplementary material Fig. S2C). In addition, mosaic animals that lost the *sra-6p::calbindin* array in ASIR had a significant bias towards AWCR^{ON} (Table 1, row w). It has not been determined whether ASI has a positive or negative influence on AWC^{ON} fate. ASIR is derived from the same lineage as AWBR and AFDR (supplementary material Fig. S1), which both inhibit AWC^{ON} (Chuang et al., 2007), so it is possible that calcium in ASIR inhibits AWCL^{ON} fate.

IP3 and serotonin signaling are not required for AWC asymmetry

Intercellular calcium waves can be propagated by movement of inositol trisphosphate (IP3) through gap junctions (Sáez et al., 1989). In addition, serotonin may move through gap junctions to coordinate the left-right body axis and modulate intercellular calcium signaling, and ADF neurons of the NSY-5 network synthesize serotonin (Blomstrand et al., 1999; Duerr et al., 1999;

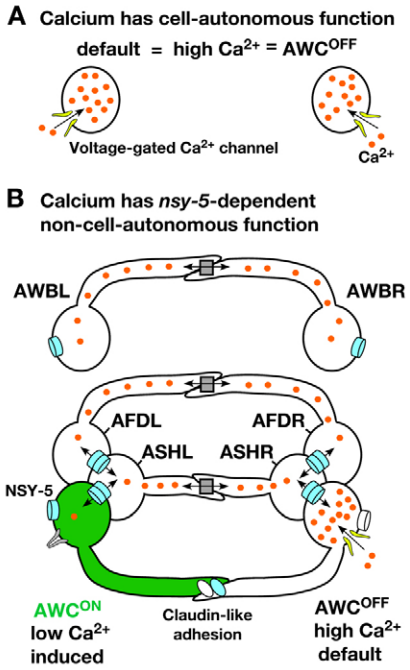

Fig. 6. Model of calcium function in left-right AWC asymmetry. (**A**) Calcium functions cell-autonomously within AWCs to promote the AWC^{OFF} fate. Both AWC cells, before cell-cell communication, have calcium influx through voltage-gated calcium channels to maintain the default AWC^{OFF} fate. (**B**) Calcium mediates intercellular signaling between non-AWCs and AWCs within the NSY-5 network to induce one AWC^{ON} and thus has a *nsy-5*-dependent non-cell-autonomous role in AWC asymmetry. The relative calcium level in the two AWC cells determines asymmetric AWC subtypes: the AWC with a lower calcium level becomes the induced AWC^{ON}, whereas the contralateral AWC with a higher level of calcium remains as the default AWC^{OFF}. AWB cells express *nsy-5*, but do not directly contact AWC. AWBs may communicate with AWCs through other cells in the NSY-5 network. Gray rectangles represent gap junctions identified from EM reconstructions of adult (White et al., 1986). Blue cylinders represent NSY-5 gap junction channels.

Zimmermann and Walz, 1999; Sze et al., 2000; Fukumoto et al., 2005a; Fukumoto et al., 2005b; Peters et al., 2005; Levin et al., 2006). To address potential roles of IP3 and serotonin in mediating AWC asymmetry, we examined AWC^{ON} induction in mutants that disrupt components of each signaling pathway. We analyzed mutants of the following genes required for IP3 signaling: *itr-1* (a single IP3 receptor), *lfe-2* (IP3 kinase), *ipp-5* (5-phosphatase) and *plc-3* (phospholipase C) (Clandinin et al., 1998; Dal Santo et al., 1999; Sze et al., 2000; Bui and Sternberg, 2002). IP3 signaling mutants did not affect AWC asymmetry (supplementary material Table S3). *C. elegans* has a single tryptophan hydroxylase (the key enzyme for serotonin biosynthesis) gene, *tph-1*, and *tph-1(mg280lf)* mutants do not synthesize serotonin (Sze et al., 2000). *tph-1(mg280lf)* mutants had wild-type AWC asymmetry (supplementary material Table S3). Together, these results suggest that IP3 and serotonin are not involved in *nsy-5*-mediated intercellular signaling for AWC asymmetry.

DISCUSSION

Discovering the nature of intercellular signaling is an important step towards understanding how groups of cells coupled by gap junctions coordinately communicate to diversify cell fates. We have taken advantage of well-characterized vertebrate calcium-buffer proteins and powerful *C. elegans* genetic tools to manipulate intracellular calcium levels selectively in individual cells or small groups of cells within the NSY-5 gap junction network to determine the non-cell-autonomous role of calcium in AWC fate diversification across the left-right axis. The genetic mosaic results revealed that calcium in non-AWC neurons of the NSY-5 network promotes wild-type 1AWC^{ON}/1AWC^{OFF} cell fate decision. In addition, calcium in AWB, ASH and ASI cells influences AWC^{ON} side biases. To our knowledge, this is the first in vivo study that directly reveals novel roles for intercellular calcium signaling within a gap junction network and dissects roles for specific cells in the network in stochastic cell-fate choice. In addition, the calcium-buffer transgenic lines represent a unique system in which to rigorously test the actual role of intracellular calcium in various neurons in directing cell-fate choice, rather than simply correlating calcium dynamics with cell-fate outcomes.

Based on the mosaic results, we propose a model in which calcium regulates AWC asymmetry by providing both cell-autonomous inputs from AWCs and non-cell-autonomous inputs from other neurons in the NSY-5 network (Fig. 6). Prior to their interaction, the two AWC neurons have spontaneous activity in order to maintain voltage-gated calcium channel-mediated signaling and the default AWC^{OFF} fate (Troemel et al., 1999; Sagasti et al., 2001; Tanaka-Hino et al., 2002; Chuang and Bargmann, 2005; VanHoven et al., 2006; Bauer Huang et al., 2007; Chuang et al., 2007) (Fig. 6A). Once the AWC cells sense each other's presence through intercellular calcium signaling between AWCs and other neurons within the NSY-5 network, calcium channels in the two AWC cells may be differentially regulated by an initial stochastic signaling event that breaks AWC symmetry. Voltage-gated calcium channels generate both calcium and voltage signals, and are subject to both calcium- and voltage-dependent activation and inactivation (Catterall, 2000). As calcium-activated signaling pathways are very sensitive to the temporal pattern of calcium signals (Thomas et al., 1996; West et al., 2001), transient differences in calcium influx between two cells can potentially generate sustained differences in calcium-regulated signaling outputs through positive- and negative-feedback mechanisms. Our results support the model that NSY-5 gap junctions transmit or modify calcium signals across the neural network, leading to differential regulation of calcium channel activity in the two AWC cells and the subsequent asymmetric differentiation of AWC cells (Fig. 6B). This extends the previous model of NSY-5 function by identifying calcium as a major mediator of intercellular communication in the NSY-5 network.

Gap junction-dependent intercellular calcium signaling has been observed in a number of different cell types and organ systems, including the neocortex, retina, airway epithelia, hepatocytes and osteoblastic cells (Sáez et al., 1989; Boitano et al., 1992; Yuste et al., 1992; Lee et al., 1994; Yuste et al., 1995; Kandler and Katz, 1998; Singer et al., 2001). One mechanism for transduction of these calcium waves is the spread of the second messenger IP3 through gap junctions, which then triggers the release of intracellular calcium stores in neighboring cells. Our results suggest that AWC asymmetry does not rely on IP3 signaling, implying an alternative mechanism for propagation of calcium signaling in the NSY-5 network. One possibility is that calcium itself travels through gap junctions to mediate intercellular communication. This type of communication is found in coupled hepatocytes, in which calcium diffusion through gap junctions may help to equalize hormonal

responses across a field of cells (Sáez et al., 1989). In addition, membrane potential is a possible signal that mediates NSY-5 gap junction intercellular communication. In support of this notion, SLO-1 and EGL-2, which represent two different classes of voltage-regulated potassium channels, also affect AWC asymmetry (Troemel et al., 1999; Sagasti et al., 2001; Davies et al., 2003).

It is clear from these results that AWC neurons integrate signals from a number of different cells both to induce AWC^{ON} and to influence AWC^{ON} side bias. In particular, the mosaic analysis in *nsy-5(lf)* mutants revealed that the calcium input from AWBR requires the presence of NSY-5 gap junctions to inhibit $AWCR^{ON}$, suggesting that there is a flow of information from AWBR to AWCR through gap junctions. AWBs do not form direct gap junctions with AWCs (Chuang et al., 2007), thus the influence from AWBs on AWCs might go through other cells in the NSY-5 network. However, it is possible that AWCR or AWCL receive inputs from additional neurons that were not included in this analysis. AWCR can respond to *nsy-5* directly but AWCL requires *nsy-5* function in multiple cells of the network (Chuang et al., 2007), suggesting that AWCL requires more inputs from neighboring cells to become AWC^{ON}. The result that $AWCL^{ON}$ is promoted by inputs from AWBR and ASHL, whereas $AWCR^{ON}$ has only the cell-autonomous input, is consistent with this.

Side-biased calcium-wave dynamics have been implicated in establishing the left-right axis in vertebrate systems. Intracellular calcium elevation on the left side of the mouse embryonic node, Hensen's node in chick, or zebrafish Kupffer's vesicle is the earliest asymmetric molecular event that is functionally linked to organ laterality (McGrath et al., 2003; Sarmah et al., 2005; Garic-Stankovic et al., 2008). Calcium may move through gap junctions to reach left side target cells, leading to activation of downstream transcription (Levin and Mercola, 1999; Hatler et al., 2009). In zebrafish, left-sided elevation of intracellular calcium transiently activates CaMKII phosphorylation, which is required for proper left-right organ placement (Francescatto et al., 2010). A similar situation might occur in AWC asymmetry. It is possible that side biases of calcium dynamics in non-AWC cells of the NSY-5 network cause elevation of calcium in one AWC and reduction of calcium in another AWC, leading to increased and decreased CaMKII activity in the future AWC^{OFF} cell and the future AWC^{ON}, respectively.

Stochastic cell-fate acquisition in the nervous system is a conserved but only partly understood phenomenon in all species (Johnston and Desplan, 2008; Losick and Desplan, 2008; Johnston and Desplan, 2010). This study suggests a novel mechanism by which stochastic neuronal diversification is established. We propose that stochastic AWC asymmetry is coordinated through competition of different AWC^{ON} side biases generated by intracellular calcium signals in non-AWCs of the NSY-5 network, in addition to previously identified intrinsic opposite biases of *nsy-4* and *nsy-5* activity in AWCs (Chuang et al., 2007).

Acknowledgements
We thank Cori Bargmann for valuable discussions and comments on the manuscript. We also thank David Richards for advice on Fluo-4 calcium imaging; Yan Zou for worm cDNA; Yutaka Yoshida for mouse cDNA; Andy Fire for *C. elegans* vectors; James Lechleiter (UT Health Science Center, San Antonio, TX) for *Parv* and *ParvCDEF* plasmids; the *C. elegans* Genetic Center for strains; and WormBase.

Funding
This work was supported by an American Cancer Society Postdoctoral Fellowship [PF-11-028-01-CSM to J.A.S.]; a National Institutes of Health (NIH) Organogenesis Training Grant [to Y.-W.H.]; NIH grants [GM084491 to M.J.A., GM077593 to W.-H.L. and RO1GM098026 to C.-F.C.]; the March of Dimes Foundation [C.C.]; Whitehall Foundation Research Awards [to C.C. and C.-F.C.]; and an Alfred P. Sloan Research Fellowship [C.-F.C.]. Deposited in PMC for release after 12 months.

Competing interests statement
The authors declare no competing financial interests.

Supplementary material
Supplementary material available online at
http://dev.biologists.org/lookup/suppl/doi:10.1242/dev.083428/-/DC1

References
Bargmann, C. I., Hartwieg, E. and Horvitz, H. R. (1993). Odorant-selective genes and neurons mediate olfaction in C. elegans. *Cell* **74**, 515-527.
Bauer Huang, S. L., Saheki, Y., VanHoven, M. K., Torayama, I., Ishihara, T., Katsura, I., van der Linden, A., Sengupta, P. and Bargmann, C. I. (2007). Left-right olfactory asymmetry results from antagonistic functions of voltage-activated calcium channels and the Raw repeat protein OLRN-1 in C. elegans. *Neural Dev.* **2**, 24.
Bennett, M. V. and Zukin, R. S. (2004). Electrical coupling and neuronal synchronization in the mammalian brain. *Neuron* **41**, 495-511.
Blomstrand, F., Khatibi, S., Muyderman, H., Hansson, E., Olsson, T. and Rönnbäck, L. (1999). 5-Hydroxytryptamine and glutamate modulate velocity and extent of intercellular calcium signalling in hippocampal astroglial cells in primary cultures. *Neuroscience* **88**, 1241-1253.
Boitano, S., Dirksen, E. R. and Sanderson, M. J. (1992). Intercellular propagation of calcium waves mediated by inositol trisphosphate. *Science* **258**, 292-295.
Brenner, S. (1974). The genetics of Caenorhabditis elegans. *Genetics* **77**, 71-94.
Bui, Y. K. and Sternberg, P. W. (2002). Caenorhabditis elegans inositol 5-phosphatase homolog negatively regulates inositol 1,4,5-triphosphate signaling in ovulation. *Mol. Biol. Cell* **13**, 1641-1651.
C. elegans Sequencing Consortium (1998). Genome sequence of the nematode C. elegans: a platform for investigating biology. *Science* **282**, 2012-2018.
Catterall, W. A. (2000). Structure and regulation of voltage-gated Ca2+ channels. *Annu. Rev. Cell Dev. Biol.* **16**, 521-555.
Chang, C., Hsieh, Y. W., Lesch, B. J., Bargmann, C. I. and Chuang, C. F. (2011). Microtubule-based localization of a synaptic calcium-signaling complex is required for left-right neuronal asymmetry in C. elegans. *Development* **138**, 3509-3518.
Chard, P. S., Bleakman, D., Christakos, S., Fullmer, C. S. and Miller, R. J. (1993). Calcium buffering properties of calbindin D28k and parvalbumin in rat sensory neurones. *J. Physiol.* **472**, 341-357.
Christensen, M., Estevez, A., Yin, X., Fox, R., Morrison, R., McDonnell, M., Gleason, C., Miller, D. M., 3rd and Strange, K. (2002). A primary culture system for functional analysis of C. elegans neurons and muscle cells. *Neuron* **33**, 503-514.
Chuang, C. F. and Meyerowitz, E. M. (2000). Specific and heritable genetic interference by double-stranded RNA in Arabidopsis thaliana. *Proc. Natl. Acad. Sci. USA* **97**, 4985-4990.
Chuang, C. F. and Bargmann, C. I. (2005). A Toll-interleukin 1 repeat protein at the synapse specifies asymmetric odorant receptor expression via ASK1 MAPKKK signaling. *Genes Dev.* **19**, 270-281.
Chuang, C. F., Vanhoven, M. K., Fetter, R. D., Verselis, V. K. and Bargmann, C. I. (2007). An innexin-dependent cell network establishes left-right neuronal asymmetry in C. elegans. *Cell* **129**, 787-799.
Clandinin, T. R., DeModena, J. A. and Sternberg, P. W. (1998). Inositol trisphosphate mediates a RAS-independent response to LET-23 receptor tyrosine kinase activation in C. elegans. *Cell* **92**, 523-533.
Dakin, K. and Li, W. H. (2006). Infrared-LAMP: two-photon uncaging and imaging of gap junctional communication in three dimensions. *Nat. Methods* **3**, 959.
Dakin, K., Zhao, Y. and Li, W. H. (2005). LAMP, a new imaging assay of gap junctional communication unveils that Ca2+ influx inhibits cell coupling. *Nat. Methods* **2**, 55-62.
Dal Santo, P., Logan, M. A., Chisholm, A. D. and Jorgensen, E. M. (1999). The inositol trisphosphate receptor regulates a 50-second behavioral rhythm in C. elegans. *Cell* **98**, 757-767.
Davies, A. G., Pierce-Shimomura, J. T., Kim, H., VanHoven, M. K., Thiele, T. R., Bonci, A., Bargmann, C. I. and McIntire, S. L. (2003). A central role of the BK potassium channel in behavioral responses to ethanol in C. elegans. *Cell* **115**, 655-666.
Duerr, J. S., Frisby, D. L., Gaskin, J., Duke, A., Asermely, K., Huddleston, D., Eiden, L. E. and Rand, J. B. (1999). The cat-1 gene of Caenorhabditis elegans encodes a vesicular monoamine transporter required for specific monoamine-dependent behaviors. *J. Neurosci.* **19**, 72-84.
Francescatto, L., Rothschild, S. C., Myers, A. L. and Tombes, R. M. (2010). The activation of membrane targeted CaMK-II in the zebrafish Kupffer's vesicle is required for left-right asymmetry. *Development* **137**, 2753-2762.

Fukumoto, T., Blakely, R. and Levin, M. (2005a). Serotonin transporter function is an early step in left-right patterning in chick and frog embryos. *Dev. Neurosci.* **27**, 349-363.
Fukumoto, T., Kema, I. P. and Levin, M. (2005b). Serotonin signaling is a very early step in patterning of the left-right axis in chick and frog embryos. *Curr. Biol.* **15**, 794-803.
Garic-Stankovic, A., Hernandez, M., Flentke, G. R., Zile, M. H. and Smith, S. M. (2008). A ryanodine receptor-dependent Ca(i)(2+) asymmetry at Hensen's node mediates avian lateral identity. *Development* **135**, 3271-3280.
Grabarek, Z. (2006). Structural basis for diversity of the EF-hand calcium-binding proteins. *J. Mol. Biol.* **359**, 509-525.
Harrisingh, M. C., Wu, Y., Lnenicka, G. A. and Nitabach, M. N. (2007). Intracellular Ca2+ regulates free-running circadian clock oscillation in vivo. *J. Neurosci.* **27**, 12489-12499.
Hatler, J. M., Essner, J. J. and Johnson, R. G. (2009). A gap junction connexin is required in the vertebrate left-right organizer. *Dev. Biol.* **336**, 183-191.
Ikura, M. (1996). Calcium binding and conformational response in EF-hand proteins. *Trends Biochem. Sci.* **21**, 14-17.
John, L. M., Mosquera-Caro, M., Camacho, P. and Lechleiter, J. D. (2001). Control of IP(3)-mediated Ca2+ puffs in Xenopus laevis oocytes by the Ca2+-binding protein parvalbumin. *J. Physiol.* **535**, 3-16.
Johnston, R. J., Jr and Desplan, C. (2008). Stochastic neuronal cell fate choices. *Curr. Opin. Neurobiol.* **18**, 20-27.
Johnston, R. J., Jr and Desplan, C. (2010). Stochastic mechanisms of cell fate specification that yield random or robust outcomes. *Annu. Rev. Cell Dev. Biol.* **26**, 689-719.
Kandler, K. and Katz, L. C. (1998). Coordination of neuronal activity in developing visual cortex by gap junction-mediated biochemical communication. *J. Neurosci.* **18**, 1419-1427.
Kumar, N. M. and Gilula, N. B. (1996). The gap junction communication channel. *Cell* **84**, 381-388.
Lee, S. H., Kim, W. T., Cornell-Bell, A. H. and Sontheimer, H. (1994). Astrocytes exhibit regional specificity in gap-junction coupling. *Glia* **11**, 315-325.
Levin, M. (2007). Gap junctional communication in morphogenesis. *Prog. Biophys. Mol. Biol.* **94**, 186-206.
Levin, M. and Mercola, M. (1999). Gap junction-mediated transfer of left-right patterning signals in the early chick blastoderm is upstream of Shh asymmetry in the node. *Development* **126**, 4703-4714.
Levin, M., Buznikov, G. A. and Lauder, J. M. (2006). Of minds and embryos: left-right asymmetry and the serotonergic controls of pre-neural morphogenesis. *Dev. Neurosci.* **28**, 171-185.
Losick, R. and Desplan, C. (2008). Stochasticity and cell fate. *Science* **320**, 65-68.
Marsh, K. A. (1995). Single-cell calcium imaging. *Methods Mol. Biol.* **41**, 229-238.
McGrath, J., Somlo, S., Makova, S., Tian, X. and Brueckner, M. (2003). Two populations of node monocilia initiate left-right asymmetry in the mouse. *Cell* **114**, 61-73.
Mello, C. and Fire, A. (1995). DNA transformation. *Methods Cell Biol.* **48**, 451-482.
Pauls, T. L., Durussel, I., Berchtold, M. W. and Cox, J. A. (1994). Inactivation of individual Ca(2+)-binding sites in the paired EF-hand sites of parvalbumin reveals asymmetrical metal-binding properties. *Biochemistry* **33**, 10393-10400.
Peters, J. L., Earnest, B. J., Tjalkens, R. B., Cassone, V. M. and Zoran, M. J. (2005). Modulation of intercellular calcium signaling by melatonin in avian and mammalian astrocytes is brain region-specific. *J. Comp. Neurol.* **493**, 370-380.
Pierce-Shimomura, J. T., Faumont, S., Gaston, M. R., Pearson, B. J. and Lockery, S. R. (2001). The homeobox gene lim-6 is required for distinct chemosensory representations in C. elegans. *Nature* **410**, 694-698.
Roayaie, K., Crump, J. G., Sagasti, A. and Bargmann, C. I. (1998). The G alpha protein ODR-3 mediates olfactory and nociceptive function and controls cilium morphogenesis in C. elegans olfactory neurons. *Neuron* **20**, 55-67.
Sáez, J. C., Connor, J. A., Spray, D. C. and Bennett, M. V. (1989). Hepatocyte gap junctions are permeable to the second messenger, inositol 1,4,5-trisphosphate, and to calcium ions. *Proc. Natl. Acad. Sci. USA* **86**, 2708-2712.
Sagasti, A., Hisamoto, N., Hyodo, J., Tanaka-Hino, M., Matsumoto, K. and Bargmann, C. I. (2001). The CaMKII UNC-43 activates the MAPKKK NSY-1 to execute a lateral signaling decision required for asymmetric olfactory neuron fates. *Cell* **105**, 221-232.
Sarmah, B., Latimer, A. J., Appel, B. and Wente, S. R. (2005). Inositol polyphosphates regulate zebrafish left-right asymmetry. *Dev. Cell* **9**, 133-145.
Shaner, N. C., Campbell, R. E., Steinbach, P. A., Giepmans, B. N., Palmer, A. E. and Tsien, R. Y. (2004). Improved monomeric red, orange and yellow fluorescent proteins derived from *Discosoma* sp. red fluorescent protein. *Nat. Biotechnol.* **22**, 1567-1572.
Shaner, N. C., Steinbach, P. A. and Tsien, R. Y. (2005). A guide to choosing fluorescent proteins. *Nat. Methods* **2**, 905-909.
Sieburth, D., Ch'ng, Q., Dybbs, M., Tavazoie, M., Kennedy, S., Wang, D., Dupuy, D., Rual, J. F., Hill, D. E., Vidal, M. et al. (2005). Systematic analysis of genes required for synapse structure and function. *Nature* **436**, 510-517.
Singer, J. H., Mirotznik, R. R. and Feller, M. B. (2001). Potentiation of L-type calcium channels reveals nonsynaptic mechanisms that correlate spontaneous activity in the developing mammalian retina. *J. Neurosci.* **21**, 8514-8522.
Sze, J. Y., Victor, M., Loer, C., Shi, Y. and Ruvkun, G. (2000). Food and metabolic signalling defects in a Caenorhabditis elegans serotonin-synthesis mutant. *Nature* **403**, 560-564.
Tanaka-Hino, M., Sagasti, A., Hisamoto, N., Kawasaki, M., Nakano, S., Ninomiya-Tsuji, J., Bargmann, C. I. and Matsumoto, K. (2002). SEK-1 MAPKK mediates Ca2+ signaling to determine neuronal asymmetric development in Caenorhabditis elegans. *EMBO Rep.* **3**, 56-62.
Taylor, R. W., Hsieh, Y. W., Gamse, J. T. and Chuang, C. F. (2010). Making a difference together: reciprocal interactions in C. elegans and zebrafish asymmetric neural development. *Development* **137**, 681-691.
Thomas, A. P., Bird, G. S., Hajnóczky, G., Robb-Gaspers, L. D. and Putney, J. W., Jr (1996). Spatial and temporal aspects of cellular calcium signaling. *FASEB J.* **10**, 1505-1517.
Troemel, E. R., Chou, J. H., Dwyer, N. D., Colbert, H. A. and Bargmann, C. I. (1995). Divergent seven transmembrane receptors are candidate chemosensory receptors in C. elegans. *Cell* **83**, 207-218.
Troemel, E. R., Kimmel, B. E. and Bargmann, C. I. (1997). Reprogramming chemotaxis responses: sensory neurons define olfactory preferences in C. elegans. *Cell* **91**, 161-169.
Troemel, E. R., Sagasti, A. and Bargmann, C. I. (1999). Lateral signaling mediated by axon contact and calcium entry regulates asymmetric odorant receptor expression in C. elegans. *Cell* **99**, 387-398.
VanHoven, M. K., Bauer Huang, S. L., Albin, S. D. and Bargmann, C. I. (2006). The claudin superfamily protein nsy-4 biases lateral signaling to generate left-right asymmetry in C. elegans olfactory neurons. *Neuron* **51**, 291-302.
Wes, P. D. and Bargmann, C. I. (2001). C. elegans odour discrimination requires asymmetric diversity in olfactory neurons. *Nature* **410**, 698-701.
West, A. E., Chen, W. G., Dalva, M. B., Dolmetsch, R. E., Kornhauser, J. M., Shaywitz, A. J., Takasu, M. A., Tao, X. and Greenberg, M. E. (2001). Calcium regulation of neuronal gene expression. *Proc. Natl. Acad. Sci. USA* **98**, 11024-11031.
White, J. G., Southgate, E., Thomson, J. N. and Brenner, S. (1986). The structure of the nervous system of the nematode Caenorhabditis elegans. *Philos. Trans. R. Soc. Lond. B* **314**, 1-340.
Yuste, R., Peinado, A. and Katz, L. C. (1992). Neuronal domains in developing neocortex. *Science* **257**, 665-669.
Yuste, R., Nelson, D. A., Rubin, W. W. and Katz, L. C. (1995). Neuronal domains in developing neocortex: mechanisms of coactivation. *Neuron* **14**, 7-17.
Zhao, Y., Zheng, Q., Dakin, K., Xu, K., Martinez, M. L. and Li, W. H. (2004). New caged coumarin fluorophores with extraordinary uncaging cross sections suitable for biological imaging applications. *J. Am. Chem. Soc.* **126**, 4653-4663.
Zimmermann, B. and Walz, B. (1999). The mechanism mediating regenerative intercellular Ca2+ waves in the blowfly salivary gland. *EMBO J.* **18**, 3222-3231.